JACS
JOURNAL OF THE AMERICAN CHEMICAL SOCIETY

Article

pubs.acs.org/JACS

Visible Light Catalysis-Assisted Assembly of Ni_h-QD Hollow Nanospheres in Situ via Hydrogen Bubbles

Zhi-Jun Li, Xiang-Bing Fan, Xu-Bing Li, Jia-Xin Li, Chen Ye, Jiu-Ju Wang, Shan Yu, Cheng-Bo Li, Yu-Ji Gao, Qing-Yuan Meng, Chen-Ho Tung, and Li-Zhu Wu*

Key Laboratory of Photochemical Conversion and Optoelectronic Materials, Technical Institute of Physics and Chemistry & University of Chinese Academy of Sciences, Chinese Academy of Sciences, Beijing 100190, People's Republic of China

Supporting Information

ABSTRACT: Hollow spheres are one of the most promising micro-/nanostructures because of their unique performance in diverse applications. Templates, surfactants, and structure-directing agents are often used to control the sizes and morphologies of hollow spheres. In this Article, we describe a simple method based on visible light catalysis for preparing hollow nanospheres from CdE (E = Te, Se, and S) quantum dots (QDs) and nickel (Ni^{2+}) salts in aqueous media. In contrast to the well-developed traditional approaches, the hollow nanospheres of QDs are formed in situ by the photogeneration of hydrogen (H_2) gas bubbles at room temperature. Each component, that is, the QDs, metal ions, ascorbic acid (H_2A), and visible light, is essential for the formation of hollow nanospheres. The quality of the hollow nanospheres depends on the pH, metal ions, and wavelength and intensity of visible light used. Of the various metal ions investigated, including Cu^+, Cu^{2+}, Fe^{2+}, Fe^{3+}, Ni^{2+}, Mn^{2+}, $RuCl_5^{2-}$, Ag^+, and $PtCl_4^{2-}$, Ni^{2+} ions showed the best ability to generate H_2 and hollow-structured nanospheres under visible light irradiation. The average diameter and shell thickness of the nanospheres ranged from 10 to 20 nm and from 3 to 6 nm, respectively, which are values rarely reported in the literature. Studies using high-resolution transmission electron microscopy (HRTEM), X-ray photoelectron spectroscopy (XPS), X-ray diffraction (XRD), inductively coupled plasma-mass spectroscopy (ICP-AES), and steady-state and time-resolved spectroscopy revealed the chemical nature of the hollow nanospheres. Additionally, the hollow-structured nanospheres exhibit excellent photocatalytic activity and stability for the generation of H_2 with a rate constant of 21 μmol h^{-1} mg^{-1} and a turnover number (TON) of 137 500 or 30 250 for CdTe QDs or nickel, respectively, under visible light irradiation for 42 h.

INTRODUCTION

In natural photosynthetic systems, light-absorbing chlorophylls are well organized in a specific geometry to form light-harvesting assemblies, and the primary light absorption and subsequent transfer of electronic excitation energy and electrons within these assemblies toward the reaction center are extremely important for the conversion of sunlight into chemical energy.[1−3] To duplicate the architecture and functionality of natural photosynthetic systems, scientists have been devoting considerable effort to developing artificial systems and exploring the energy and electron transfer functions of natural solar energy conversion systems.[4,5] An abundance of accumulated evidence has demonstrated that the organization of elegant architectures, such as organic micelles,[6] vesicles,[7−9] and inorganic hollow spheres,[10−12] is promising for light-harvesting and charge transfer in artificial photosynthetic systems and can be accessible through versatile fabrication techniques. In general, organic micelles and vesicles are constructed from surfactants or block copolymers that possess intrinsic differences in the chemical potentials of the hydrophobic/hydrophilic regions of the surfactant or polymer blocks.[13] Conversely, inorganic hollow spheres are often prepared using various sacrificial templates, including polystyrene spheres, silica spheres, resin spheres, vesicles, liquid droplets, and microemulsion droplets.[13−16] The most com-

Received: January 4, 2014

dx.doi.org/10.1021/ja5047236 | J. Am. Chem. Soc. XXXX, XXX, XXX−XXX

monly used method is a multistep process, in which the removal of the core template or two immiscible liquid phases using calcination or dissolution is technically complicated.[17]

The light-assisted method has recently become a new strategy for fabricating unique structured nanomaterials. For example, Kotov et al.[18] reported a light-controlled self-assembly method for preparing twisted ribbons using CdTe nanoparticles. Suib et al.[19] developed a self-templating method that uses UV-light to synthesize γ-manganese oxide (γ-MnO_2), cobalt oxyhydroxide (CoOOH), and cerium oxide (CeO_2) hierarchical nanoarchitectures. Fan et al.[20] employed densely packed optically active porphyrins to prepare well-defined hollow platinum (Pt) nanostructures. Here, we present a simple approach for creating hollow-structured nanospheres of quantum dots (QDs) using visible light catalysis.

Semiconductor QDs have attracted widespread attention because their nanoscale physical properties are quite different from those of bulk materials.[21,22] Because of their light absorption and large extinction coefficients over a broad spectral range, rich surface binding properties, and high surface-to-volume ratios, QDs are ideal for light-harvesting and charge separation applications.[23−34] QDs are expected to be a versatile type of building block for creating hollow structures such as those found in natural light-harvesting antenna complexes. However, few examples of these QD assemblies have been reported,[12] and the salient features associated with their assembly are unclear.

In this Article, we demonstrate that hollow-structured nanospheres of QDs can be easily synthesized in a one-pot, visible light-catalyzed reaction under ambient conditions. In contrast to well-developed methods that use polymer latex, silica, and emulsion/microemulsion as templates,[13,15,16] the hollow nanospheres are formed in situ via H_2 gas bubbles. Upon visible light irradiation of an aqueous solution that contains QDs, ascorbic acid (H_2A), and nickel (Ni^{2+}) salts at pH 4.65, the QDs are capable of assembling around the gas−liquid interface to form hollow-structured nanospheres. The absence of any of the components, that is, QDs, Ni^{2+} ions, H_2A, or visible light, resulted in no appreciable Ni_h-QDs assembly. Furthermore, the quality of the hollow nanospheres depended on the wavelength and intensity of the visible light used. Various metal ions, such as Cu^+, Cu^{2+}, Fe^{2+}, Fe^{3+}, Mn^{2+}, $RuCl_5^{2-}$, Ag^+, and $PtCl_4^{2-}$, exhibited different behaviors in the formation of hollow-structured nanospheres and in the photocatalytic generation of H_2. Of the metal ions studied, Ni^{2+} ions possessed the best ability to generate H_2 and hollow-structured nanospheres under visible light irradiation. The average diameter and shell thickness of the nanospheres ranged from 10−20 nm and 3−6 nm, respectively. These types of small-sized hollow nanospheres are rarely observed in the literature.[35] Notably, the nanospheres exhibited excellent photocatalytic activity and stability for H_2 generation. Here, the QDs serve as antenna chromophores to harvest light, and earth-abundant Ni^{2+}-centered complexes formed in situ with dangling bonds (Te^{2-}, S^{2-}) on the surface of the QDs serve as reaction centers to capture the photoexcited electrons of the QDs for H_2 generation. Consequently, Ni_h-CdTe hollow nanospheres, for example, enable the photogeneration of H_2 from an aqueous H_2A solution with a rate constant of 21 μmol h^{-1} mg^{-1} and a TON of 75 000 or 16 500 for CdTe QDs or nickel (referring to 0.16 wt % nickel, ICP-AES), respectively, under visible light irradiation for 21 h. No obvious variation was observed in the rate of H_2 formation in one continuous irradiation cycle. The current study clearly not only offers an attractive method for assembling advanced hollow QD architectures similar to those found in natural photosynthetic systems, but also provides robust artificial photocatalysts to realize the practical production of solar fuels.

RESULTS AND DISCUSSION

Ni_h-CdTe Hollow Nanosphere Preparation and Characterization. The Ni_h-CdTe hollow nanospheres were synthesized in an aqueous solution of 3-mercaptopropionic acid (MPA)-stabilized CdTe QDs, $NiCl_2{\cdot}6H_2O$, and H_2A at room temperature. Because MPA-capped CdTe QDs (Figures S1,S2, see details in the Supporting Information) are extremely sensitive to the pH of the solution, we kept the initial pH value of the solution approximately to the pK_a of H_2A at 4.65.[36] During irradiation (λ > 400 nm), the solution became colorless with the formation of precipitates. However, no change was observed when the same solution was kept in the dark. Evidently, the precipitates resulted from visible light irradiation, and the photochemical reaction occurred on the surface of the MPA-CdTe QDs rather than in the solution.

Examination of the precipitates by HRTEM revealed that uniform hollow nanospheres were formed at a large scale after irradiation (Figure 1a−c). Unlike the MPA-CdTe QDs (Figure 1d), the average size of the hollow structure ranged from 10 to 20 nm, and its shell thickness ranged from 3 to 6 nm. However, the typical lattice plane distance of 3.52 Å (Figure 1c) is identical to that of CdTe QDs[37,38] (Figure 1d). The well-defined diffraction spots exhibited three obvious diffraction

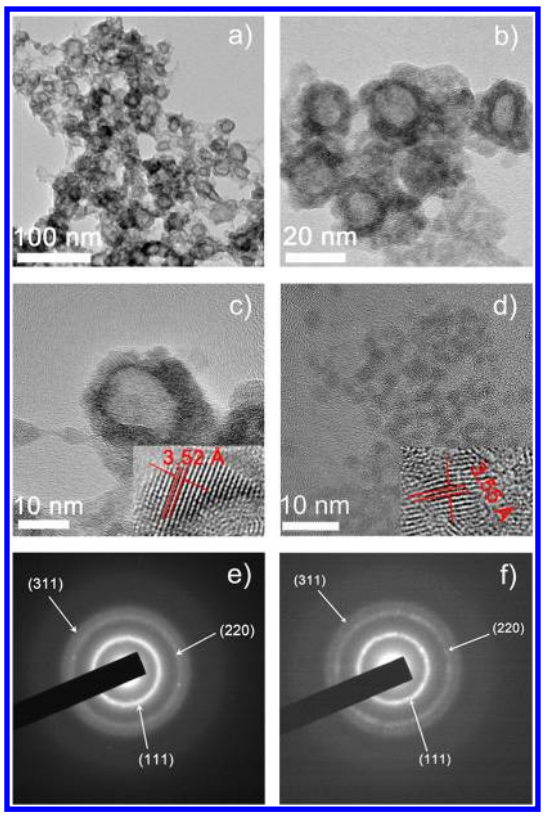

Figure 1. HRTEM images of Ni_h-CdTe hollow nanospheres (a−c) (scale bars: a, 100 nm; b, 20 nm; c, 10 nm), and their SAED pattern (e) with three diffraction rings; HRTEM image of the MPA-CdTe QDs (d), and their SAED pattern (f) with three diffraction rings.

dx.doi.org/10.1021/ja5047236 | J. Am. Chem. Soc. XXXX, XXX, XXX−XXX

rings corresponding to the (111), (220), and (311) lattice planes, respectively (Figure 1e), which is consistent with typical CdTe QDs (Figure 1f). All of the results suggested that the crystalline structure of the shell of the nanospheres is composed of CdTe QDs. The as-obtained hollow nanospheres were generated in situ via the assembly of small CdTe QDs rather than through the Ostwald ripening process.[14,16]

The in situ assembly of the hollow-structured nanospheres was further characterized using XRD. The average size of the corresponding lattice plane (111) was estimated to be 3.4 nm using the Debye–Scherrer formula,[39] and this value is similar to that of the MPA-CdTe QDs determined using HRTEM (Supporting Information Figure S2). Although the shapes and widths of the three peaks shown in Figure 2 negligibly changed

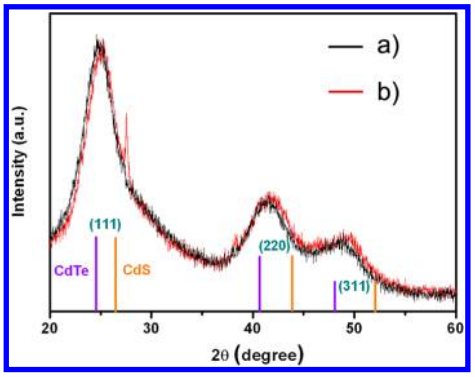

Figure 2. XRD patterns of (a) MPA-CdTe QDs and (b) Ni_h-CdTe hollow nanospheres.

as a result of the aggregation of the CdTe QDs, their positions moved slightly toward higher angles as compared to those of MPA-CdTe QDs (bulk cubic (zinc blende) CdTe, International Centre for Diffraction Data, JCPDS card no. 65-1046). The higher shift of the diffraction pattern of the hollow nanospheres toward that of CdS (bulk cubic (zinc blende) CdS, JCPDS card no. 10-0545) may be a result of the partial decomposition of MPA during illumination leading to the incorporation of CdS on the surface of the CdTe nanocrystals,[40] which is consistent with the increment of sulfur species in the CdTe QDs after irradiation (confirmed by ICP-AES, see Supporting Information Table S1).

To determine the exact chemical composition and electronic structure, the XPS spectrum was carefully investigated. Note that the electron binding energy depends not only on the element it comes from but also on the chemical state of the element in the given nanoparticles (Figure 3).[41,42] The peak at approximately 162 eV arises from S 2p with a doublet structure, corresponding to S $2p_{1/2}$ and S $2p_{3/2}$, which are separated by 1.3 eV.[43] Before irradiation, the XPS spectrum of the MPA-CdTe QDs could be well fit with one doublet for S $2p_{1/2}$ at 162.95 eV and S $2p_{3/2}$ at 161.65 eV, which suggests the existence of chemical bonds between the thiols of MPA and the cadmium ions on the surface of the CdTe QDs.[44] After irradiation, the S 2p doublet increased significantly and shifted to a lower binding energy. A new doublet peak at 162.25 eV for S $2p_{1/2}$ and at 161.23 eV for S $2p_{3/2}$ implied that irradiation leads to the decomposition of MPA to CdS.[40] Thus, the photodecomposition process resulted in changes in the chemical properties of the CdTe QDs. Additionally, the Ni signals from the hollow-structured nanospheres were detected using XPS (Supporting Information Figure S3). Despite being

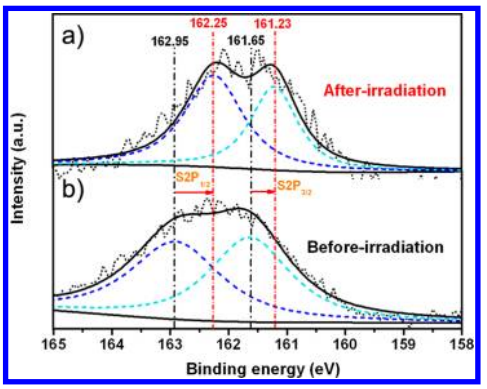

Figure 3. S 2p XPS spectra recorded from (a) Ni_h-CdTe hollow nanospheres and from (b) MPA-CdTe QDs; the vertical lines are guides for the positions of S $2p_{1/2}$ and S $2p_{3/2}$ from MPA-Cd and CdS, respectively.

weak, a Ni(II) $2p_{3/2}$ peak at ca. 854.8 eV and a Ni(II) $2p_{1/2}$ peak at ca. 871.4 eV[45,46] were clearly observed. Furthermore, the amount of Ni was determined to be 0.16 wt % using the ICP-AES method (Supporting Information Table S1).

Following the same method, Ni_h-CdSe and Ni_h-CdS hollow-structured nanospheres were successfully synthesized using MPA-CdSe QDs and MPA-CdS QDs, respectively (Supporting Information Figure S4). The average size (10–20 nm) and shell thickness (3–6 nm) of the obtained hollow structures are difficult to realize using external templates. With unique structural characteristics, the hollow-structured nanospheres of the QDs could provide a rich platform for exploring new functional materials.

Mechanistic Insight into the Formation of Hollow-Structured Nanospheres. To determine the factors that control the formation of hollow-structured nanospheres, a set of parallel experiments were carefully conducted. It was determined that MPA-QDs, $NiCl_2 \cdot 6H_2O$, H_2A, and visible light are all essential to formation of hollow nanospheres. The absence of any of these components resulted in no appreciable Ni_h-QDs assembly, including that of Ni_h-CdTe (Supporting Information Figures S5,S6). Furthermore, commercially available CdTe powders were investigated for comparison, but no hollow nanospheres were obtained under identical conditions. This finding confirms that the unique characteristics of MPA-CdTe QDs are considerably different than those of bulk materials.

The formation of the Ni_h-CdTe hollow nanospheres was strongly dependent on the pH of the solution (Figure 4). When the pH was <4, only aggregates of CdTe QDs were observed. When the pH was >4, Ni_h-CdTe hollow nanospheres formed with variable quality. The highest quality Ni_h-CdTe hollow nanospheres were formed at pH 4.65 (Figure 4).

Because no additive or template was used in any part of the process, we examined the photoproducts of the reaction system in addition to the hollow-structured nanospheres. Notably, H_2 was detected as the only product in the reaction mixture. In this situation, it can be assumed that the hollow nanospheres are a result of the assemblies around the gas–liquid interface of the H_2 gas bubbles generated in situ in water.[14,15] This assumption was well corroborated by the fact that a higher H_2 photogeneration efficiency led to higher quality hollow nanospheres. A sharp maximal rate for H_2 evolution was observed at pH 4.65 (Supporting Information Figure S7), while significant amounts of H_2 were also obtained at lower or higher

dx.doi.org/10.1021/ja5047236 | J. Am. Chem. Soc. XXXX, XXX, XXX–XXX

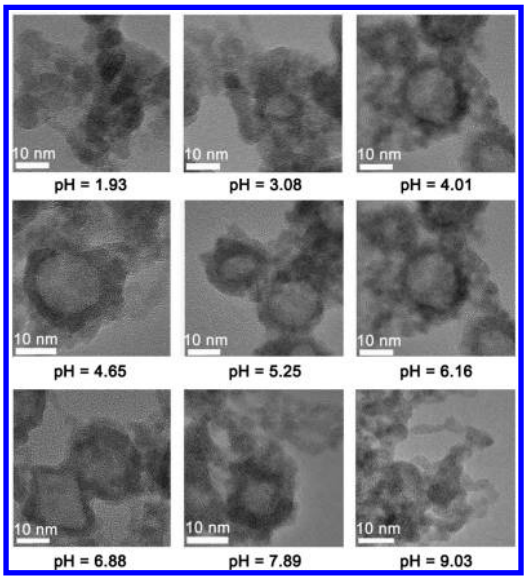

Figure 4. HRTEM images of hollow Ni_h-CdTe nanospheres obtained at different pH values (scale bar: 10 nm).

pH values. Furthermore, the same trend was observed in the formation of Ni_h-CdTe hollow-structured nanospheres (Figure 4).

To examine the general applicability of the approach studied in this work, we used other metal ions available in our laboratory to clarify the formation of hollow-structured nanospheres and the photocatalytic generation of H_2. As shown in Figure 5, various metal ions, such as Cu^+, Cu^{2+}, Fe^{2+}, Fe^{3+}, Mn^{2+}, $RuCl_5^{2-}$, Ag^+, and $PtCl_4^{2-}$, with different valence states and reduction potentials (Supporting Information Table S2) exhibit different behaviors. With the irradiation of an aqueous solution containing MPA-CdTe QDs, metal ions, and H_2A at pH 4.65, only the Ni^{2+}, Fe^{2+}, and Fe^{3+} ions that evolve H_2 are noticeably capable of forming the hollow-structured nanospheres (Figures 1 and 5). Of the metal ions studied, Ni^{2+} ions were found to possess the best ability to generate H_2 and hollow nanospheres under visible light irradiation. For the metal ions that gave rise to small amounts or no H_2 evolution from the system, that is, Mn^{2+}, Cu^+, Cu^{2+}, $RuCl_5^{2-}$, Ag^+, and $PtCl_4^{2-}$, only aggregates of CdTe QDs were observed (Figure 5). All of these results demonstrate that the photogeneration of H_2 bubbles in situ is essential for assembling QDs into hollow-structured nanospheres.

In addition to the facile morphology control offered by the optimal pH and metal ions of the reaction system, the quality of hollow-structured nanospheres also depends on the wavelength and intensity of visible light used (Figure 6). When monitoring a specific wavelength of incident visible light from an LED (410, 455, 530, 590, and 630 nm; 80 mW cm^{-2}), we observed that the only light wavelengths that QDs absorb are 410, 455, and 530 nm, which provide good to excellent performance for the generation of H_2 gas bubbles and thus lead to the formation of high-quality hollow nanospheres of QDs (Figure 6). Moreover, the light intensity (410 nm LED, 160 mW cm^{-2}, 80 mW cm^{-2}, and 40 mW cm^{-2}) for a given reaction system also significantly influenced the quality of the hollow nanospheres, which is related to the same trend of H_2 evolution activity (Supporting Information Figure S8).

In an effort to understand the entire process, we further studied the interaction of the necessary components: Ni^{2+} ions, H_2A, and MPA-CdTe QDs. For the solutions at pH 11 and pH 4.65, the MPA-CdTe QDs exhibited zeta potentials of -40.6 ± 1.6 and -13.8 ± 0.7 mV, respectively. The negative zeta potential values along with the FT-IR spectral study (Supporting Information Figure S9) identified the negatively charged surface, which depends on the degree of deprotonation of the carboxyl groups and on the surface dangling bond (Te^{2-}, S^{2-}) of QDs (see details in the Supporting Information). When $NiCl_2 \cdot 6H_2O$ was added to the aqueous solution of MPA-CdTe QDs, the band edge emission was dramatically quenched (Figure 7a) with a shortened lifetime (Supporting Information Figure S10), which suggested that the interaction of the MPA-CdTe QDs and Ni^{2+} ions was in the excited state. The linear plot of the Langmuir law[47] indicated that Ni^{2+} ions were binding to the surface dangling bond (Te^{2-}, S^{2-}) of the QDs[30,39,47,48] (Supporting Information Figure S11) to form a Ni^{2+}-centered complex in situ with Te^{2-} and S^{2-} ligands,[29,46] as described by Talapin et al.[48,49]

Because the conduction band energy level (E_{cb}) of the MPA-CdTe QDs (3.4 nm) (−1.6 V vs NHE)[25] is more negative than the redox potential of the Ni^{2+}/Ni^0 couples (−0.25 V vs NHE),[50] the free energy change of the electron transfer from the excited MPA-CdTe QDs to the Ni^{2+} ions is thermodynamically favorable. The photoinduced electron transfer process was directly investigated using a nanosecond transient absorption

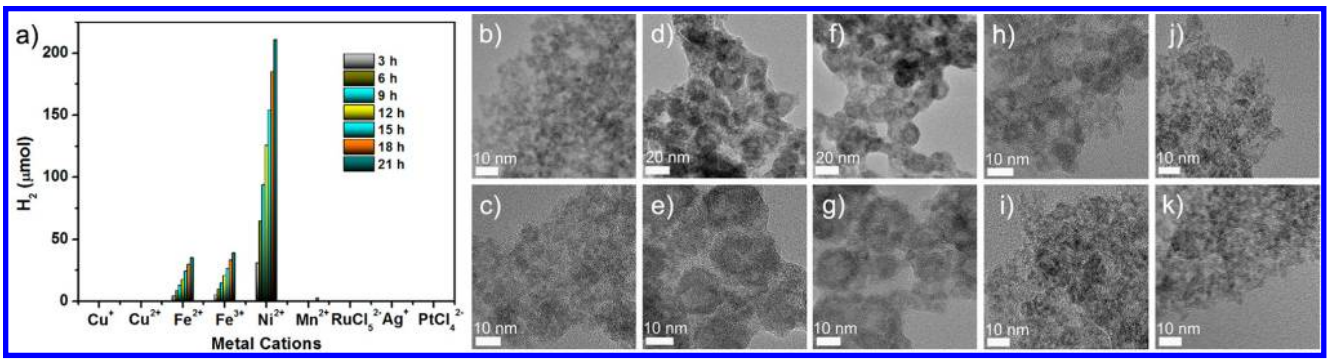

Figure 5. Visible light catalysis-assisted assembly of hollow nanospheres and H_2 generation using other metal ions: (a) Time course of H_2 evolution from MPA-CdTe QDs (2.4×10^{-7} M), H_2A (2.84×10^{-2} M), and metal ions (2.1×10^{-4} M), Cu^+, Cu^{2+}, Fe^{2+}, Fe^{3+}, Ni^{2+} (as a reference), Mn^{2+}, $RuCl_5^{2-}$, Ag^+, and $PtCl_4^{2-}$ suspended in 5 mL of an aqueous solution (pH = 4.65) under monochromated light from a 410 nm LED; HRTEM images of the precipitates obtained from the reaction system with various metal ions, (b) Cu^+, (c) Cu^{2+}, (d,e) Fe^{2+}, (f,g) Fe^{3+}, (h) Mn^{2+}, (i) $RuCl_5^{2-}$, (j) Ag^+, and (k) $PtCl_4^{2-}$.

dx.doi.org/10.1021/ja5047236 | J. Am. Chem. Soc. XXXX, XXX, XXX−XXX

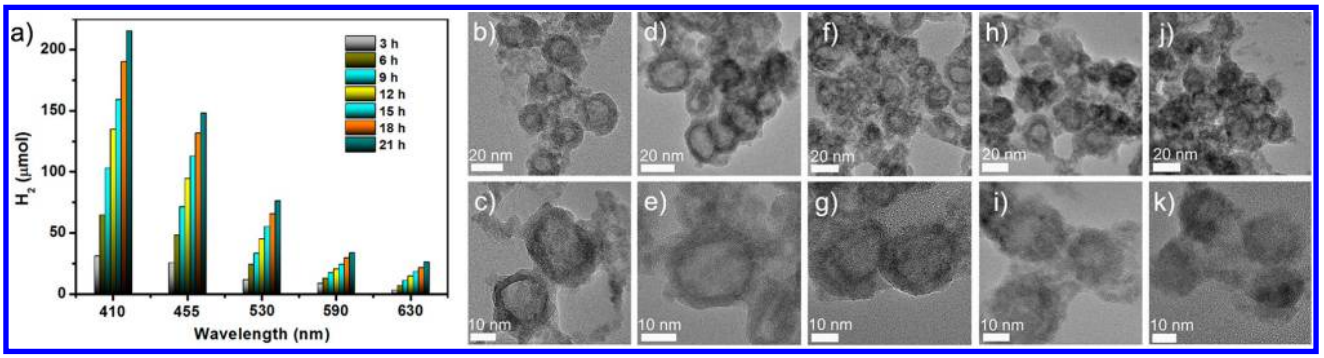

Figure 6. Visible light wavelength dependence of H_2 evolution and Ni_h-CdTe hollow nanosphere formation: (a) Time course of H_2 evolution, $NiCl_2 \cdot 6H_2O$ (2.1×10^{-4} M), MPA-CdTe QDs (2.4×10^{-7} M), and H_2A (2.8×10^{-2} M) suspended in 5 mL of an aqueous solution (pH = 4.65) under monochromated light from an LED at 410, 455, 530, 590, and 630 nm; HRTEM images of the hollow nanospheres obtained at specific light irradiation wavelengths for 21 h, (b,c) 410 nm, (d,e) 455 nm, (f,g) 530 nm, (h,i) 590 nm, and (j,k) 630 nm.

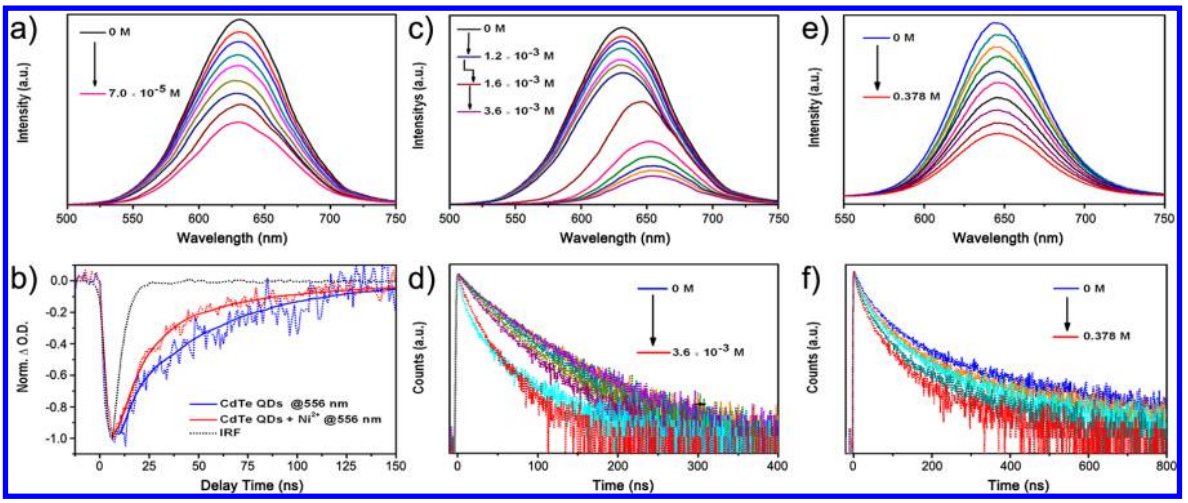

Figure 7. Emission spectra of the MPA-CdTe QDs (2.4×10^{-7} M) with a concentration of (a) $NiCl_2 \cdot 6H_2O$ (0 to 7.0×10^{-5} M), (c) H_2A (0 to 3.6×10^{-3} M), and (e) H_2A (0 to 0.378 M) at pH = 4.65 in water; (b) nanosecond recovery kinetics of bleaching for MPA-CdTe QDs in the absence and presence of Ni^{2+} ions monitored at 556 nm and normalized to the maximal signal. The fits were deconvolved with a Gaussian function with a 4 ns fwhm representing the instrument response; emission decays of the MPA-CdTe QDs (2.4×10^{-7} M) with various concentrations of (d) H_2A (0 to 3.6×10^{-3} M), and (f) H_2A (0 to 0.378 M) at pH = 4.65 in water (excitation wavelength: 406 nm).

study. After being laser-pulsed at 410 nm, the MPA-CdTe QDs displayed a kinetic decay of the characteristic absorption (556 nm) with a lifetime of 46.2 ns. When Ni^{2+} ions were introduced into the solution, the lifetime of the absorptions decreased to 26.8 ns, which is shorter than that of the CdTe QDs alone (τ = 46.2 ns) (Figure 7b). The faster recovery of exciton bleaching in the presence of Ni^{2+} ions suggested an effective electron transfer from the excited MPA-CdTe QDs to the Ni^{2+} active sites,[51] a crucial step in the photogeneration of H_2 gas (see details in the Supporting Information) and the subsequent in situ assembly process.

On the other hand, the addition of H_2A to the MPA-CdTe QD solution led to a remarkable decrease in the emission intensity and lifetime (Figure 7c,d), which is a result of the protonation or detachment of the MPA from the QDs, causing aggregation of soluble QDs.[52,53] The red-shift in the emission spectra (Figure 7c) but not in the absorption spectra (Supporting Information Figure S12) could be explained by the fact that the energy transfers from the aggregated smaller MPA-CdTe QDs (larger band gap due to the quantum confinement effect) to the larger ones (smaller band gap).[53−56] To avoid the interference of further aggregation and energy transfer of the suspended QDs, we used hydrochloride (HCl) to adjust the solution pH to 4.65 and then determined the interaction between the CdTe QDs and H_2A.[51,57] As shown in Figure 7e, introducing H_2A to an aqueous solution of CdTe QDs significantly quenched the band edge emission. In the absence and presence of H_2A, the lifetime of the emission decreased by a factor of ~2 from 81.8 to 40.1 ns (Figure 7f), which was attributed to the photogenerated holes trapped by the H_2A. Neither the Ni_h-CdTe hollow nanospheres nor H_2 were obtained when H_2A was replaced by HCl (Supporting Information Figures S5,S6), indicating that the hole transfer from the CdTe QDs to H_2A is also important. Here, H_2A (a weak dibasic acid in aqueous solution[58]) serves not only as a proton source for H_2 production but also as a sacrificial electron donor for regenerating QDs after the photoinduced electron transfer.

On the basis of the above results and analyses, a potential mechanism for the formation of Ni_h-CdTe hollow-structured nanospheres can be proposed. First, the negative surface dangling bonds (Te^{2-}, S^{2-}) on the surface of the CdTe QDs interact with positively charged Ni^{2+} ions to form a Ni_h-QD photocatalyst in situ,[30,48] which has a tendency to aggregate in the presence of H_2A. Upon visible light irradiation of the Ni_h-QDs, electron transfer from the excited QDs to the Ni^{2+}-

dx.doi.org/10.1021/ja5047236 | J. Am. Chem. Soc. XXXX, XXX, XXX−XXX

centered complex occurs. The reduced Ni^{2+}-centered complex further reacts with protons to generate H_2. On the other hand, the formed hole that remains in the Ni_h-QDs after the electron transfer is regenerated by the sacrificial electron donor of H_2A. Consequently, the catalytic cycle for the evolution of H_2 is achieved, the detailed mechanism of which is presented in the Supporting Information (Scheme S1). Notably, the H_2 bubbles generated in situ under visible light irradiation may act as the center of the Ni_h-QDs assembly. Driven by the minimization of interfacial energy[14,59−61] and the photodecomposition of MPA,[30,40] the aggregated Ni_h-QDs are organized around the gas−liquid interface of H_2 bubbles to form hollow-structured nanospheres of Ni_h-CdTe to scale. On the basis of the size and shell thickness of the nanospheres, the number of QD units in one hollow nanosphere was calculated to range from 95 to 286 (see details in the Supporting Information). In contrast to the traditional gas bubble template methods[59−66] that use specific physical processes[66] or thermochemical reactions,[67] the superiority of the current approach is the ability to prepare hollow nanospheres using H_2 bubbles generated in situ by visible light catalysis. The shell thickness of 3−6 nm, which corresponds to the monolayer to bilayer of the CdTe QDs (the diameter is 3.4 nm), and the dimensions of <20 nm are rarely realized in the preparation of hollow spheres.[13−16,35]

Photocatalytic Activity of Ni_h-QD Hollow Nanospheres. The appealing architecture and function of the hollow-structured nanospheres are similar to that observed in the photosynthetic reaction center for storing sunlight as chemical energy in the form of H_2. When the Ni_h-CdTe hollow nanospheres (referring to 0.16 wt % nickel, ICP-AES) were dissolved in an aqueous H_2A solution (5.68×10^{-2} M, 10 mL, pH 4.65), for example, the rate of H_2 production (~21 μmol h^{-1} mg^{-1}, 180 μmol of H_2) was nearly linear even after 21 h of irradiation by visible light, and the TON approached 75 000 or 16 500 for MPA-CdTe QDs or nickel, respectively (see TON determination in the Supporting Information). One continuous irradiation cycle was conducted to examine the reproducibility of each photocatalyst bed (Figure 8). No apparent variation in the rate of H_2 formation was observed throughout the irradiation process. The amount of H_2 was evaluated as an average value from two cycles. More than 330 μmol of H_2 (TON of 137 500 or 30 250 for CdTe QDs or nickel, respectively) was produced during the course of 42 h of irradiation. The internal quantum efficiency (IQE, see details in the Supporting Information) is a function of the visible light wavelength used (410 nm, 455 nm, 530 nm, 590 nm, 630 nm; 80 mW cm^{-2}) (Supporting Information Figure S13), and the highest IQE was determined to be 1.8% at 455 nm. These results greatly motivate us to construct hollow-structured nanospheres as effective and robust artificial photosynthetic systems for H_2 generation.

CONCLUSION

In summary, we have developed a new approach to create hollow nanoarchitectures of Ni_h-CdTe QDs, where water-soluble MPA-CdTe QDs, Ni^{2+} ions, and H_2A serve as the subcomponents. The absence of any of the components, that is, QDs, Ni^{2+} ions, H_2A, or visible light, resulted in no appreciable amount of the Ni_h-QD hollow-structured nanospheres. The quality of the hollow nanospheres depends on the wavelength and intensity of the visible light used. Various metal ions, such as Cu^+, Cu^{2+}, Fe^{2+}, Fe^{3+}, Mn^{2+}, $RuCl_5^{2-}$, Ag^+, and $PtCl_4^{2-}$, exhibited different behaviors for the formation of the hollow nanospheres and in the photocatalytic generation of H_2. Of the metal ions studied, Ni^{2+} ions possessed the best ability to generate H_2 and hollow-structured nanospheres. Under visible light irradiation, the hollow nanospheres can be successfully created via H_2 gas bubbles generated in situ, rather than using external templates. The average diameter and shell thickness of the nanospheres range from 10−20 nm and 3−6 nm, respectively. These types of small-sized hollow spheres are rarely observed in the literature.[35] Although QDs have been demonstrated to be excellent building blocks for assembling ordered structures, the challenge still remains to achieve hierarchical architectures using bubble templates, especially bubbles generated in situ through chemical reactions. The strategy presented here is general and can be extended to other cadmium chalcogenides (CdE; E = Se, S) and metal salts under ambient conditions. By taking advantage of visible light catalysis, this novel method offers an attractive one-pot route for the fabrication of advanced functionalized materials for artificial photosynthetic devices. The mechanistic information will help us design various hollow nanospheres capable of light-harvesting, charge separation, and catalysis, which occur in natural photosynthesis systems.

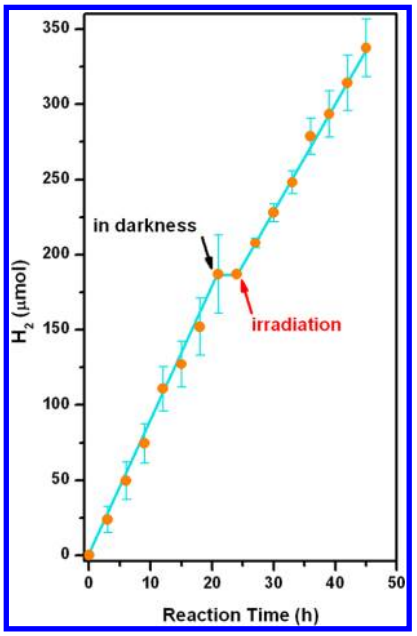

Figure 8. Photosynthetic H_2 production from Ni_h-CdTe hollow nanospheres in 10 mL of a 5.68×10^{-2} M (100 mg/10 mL) H_2A aqueous solution (pH = 4.65) under visible light irradiation (λ > 400 nm). Error bars represent the mean ± s.d. of three independent experiments.

EXPERIMENTAL SECTION

Preparation of Sodium Hydrogen Telluride. The reported method for preparing sodium hydrogen telluride (NaHTe)[68] was used with some modifications. Briefly, 80 mg of sodium borohydride was transferred to a small flask. Next, 1 mL of ultrapure water was added. After 127.5 mg of tellurium powder was added to the flask, the reaction system was cooled using ice. A small outlet connected to the flask was kept open to discharge the pressure from the hydrogen generated during the reaction. Within 3−5 h, the black tellurium powder generally disappeared, and a white sodium tetraborate precipitate appeared on the bottom of the flask. The resulting NaHTe in the supernatant was separated to prepare the CdTe particles.

dx.doi.org/10.1021/ja5047236 | J. Am. Chem. Soc. XXXX, XXX, XXX−XXX

Synthesis of Water-Soluble MPA-CdTe QDs. An aqueous colloidal MPA-CdTe QDs solution was prepared using the reaction between Cd^{2+} and NaHTe solutions according to the literature.[68] The Cd^{2+} precursor solutions were prepared by mixing solutions of $CdCl_2 \cdot 2.5H_2O$ and stabilizer (MPA) followed by a pH adjustment to 11 with 1 M NaOH. The typical molar ratio of Cd:MPA:Te was maintained at 1:1.2:0.2 in our experiment. This solution was placed in a three-necked flask, which was fitted and deaerated with N_2 bubbling, for 30 min. The resulting solution was then heated to 99−100 °C and refluxed for different reaction times to control the sizes of the MPA-CdTe QDs. Aliquots of the reaction solution were collected at regular intervals for characterization via UV−vis absorption and emission.

General Procedure for the Preparation of Ni_h-CdTe Hollow Nanospheres. An aqueous colloidal MPA-CdTe solution (2.4×10^{-7} M, 0.4 mg/10 mL), H_2A (2.84×10^{-2} M, 50 mg/10 mL), and $NiCl_2 \cdot 6H_2O$ (2.1×10^{-4} M, 0.5 mg/10 mL) were added to a Schlenk tube. The total volume of each sample was 10 mL. Prior to irradiation, the pH value of the solution was adjusted using an aqueous 1.0 M NaOH or 1.0 M HCl solution and verified using a pH meter. The sample was degassed by bubbling nitrogen for 30 min and then irradiated under a high-pressure Hanovia mercury lamp (light intensity of 100 mW cm^{-2} at the Schlenk tube surface) with a light wavelength longer than 400 nm.

For the conditioning experiments on metal ions and light wavelength and intensity, an aqueous colloidal MPA-CdTe solution (2.4×10^{-7} M, 0.2 mg/5 mL), H_2A (2.84×10^{-2} M, 25 mg/5 mL), and metal ions (Cu^+, Cu^{2+}, Fe^{2+}, Fe^{3+}, Ni^{2+}, Mn^{2+}, $RuCl_5^{2-}$, Ag^+, and $PtCl_4^{2-}$ (2.1×10^{-4} M)) were added to a Schlenk tube. The total volume of each sample was 5 mL. Prior to irradiation, the pH value of the solution was adjusted to 4.65 using an aqueous 1.0 M NaOH or 1.0 M HCl solution and verified using a pH meter. The sample was degassed by bubbling nitrogen for 30 min and then irradiated under monochromated light from an LED (80 mW cm^{-2}) at 410, 455, 530, 590, or 630 nm or under varied light intensity (monochromated light from a 410 nm LED, 160 mW cm^{-2}, 80 mW cm^{-2}, and 40 mW cm^{-2}).

The suspension of the QDs tends to form precipitates because the protonation of MPA (the thiol group) results in a partial dissociation of the ligand from the QD surface under acidic conditions combined with irradiation ($\lambda > 400$ nm). To overcome this problem, the H_2 evolution experiment was performed under rapidly rigorous stirring to maintain the QDs in suspension. The generated photoproduct of H_2 was characterized by GC analysis (Techcomp 7890-II) using nitrogen as the carrier gas with a molecular sieve column (5 Å) and a thermal conductivity detector. After 21 h of irradiation, we isolated the QD precipitates from the solution using centrifugation, and each component was further dispersed using ultrasonication. The samples then were prepared for HRTEM observation by dropping dispersed suspended precipitates onto ultrathin carbon-coated copper grids with the excess solvent evaporated.

General Procedure for Photocatalytic H_2 Generation. The Ni_h-CdTe hollow nanospheres, which were formed from a system containing $NiCl_2 \cdot 6H_2O$ (2.1×10^{-4} M, 0.5 mg/10 mL), the MPA-CdTe QDs (2.4×10^{-7} M, 0.4 mg/10 mL), and H_2A (2.84×10^{-2} M, 50 mg/10 mL) in water at pH 4.65 under visible light irradiation (21 h, $\lambda > 400$ nm), were obtained by centrifugation and immediately added to 10 mL of a 5.68×10^{-2} M (100 mg/10 mL) H_2A aqueous solution (pH = 4.65). CH_4 (500 μL in concentration effect, control experiments, and optimized concentration experiments to ensure that sufficient CH_4 was extracted from the samples) was injected as the internal standard for quantitative GC analysis. The sample was then irradiated under a high-pressure Hanovia mercury lamp (light intensity of 100 mW cm^{-2} at the Schlenk tube surface) with a light wavelength longer than 400 nm. The generated photoproduct of H_2 was characterized through GC analysis (Techcomp 7890-II) using nitrogen as the carrier gas with a molecular sieve column (5 Å) and a thermal conductivity detector. Five hundred microliters of mixed gas was extracted from the sample tube and immediately injected into the GC. The response factor for H_2/CH_4 was approximately 4.86 under the experimental conditions, which was established by calibration with known amounts of H_2 and CH_4 and determined before and after a series of measurements.

■ ASSOCIATED CONTENT

Ⓢ Supporting Information

Additional experimental details, Tables S1,S2, and Figures S1−S13. This material is available free of charge via the Internet at http://pubs.acs.org.

■ AUTHOR INFORMATION

Corresponding Author

lzwu@mail.ipc.ac.cn

Notes

The authors declare no competing financial interest.

■ ACKNOWLEDGMENTS

We are grateful for the financial support from the Ministry of Science and Technology of China (2013CB834505, 2014CB239402, and 2013CB834804), the National Natural Science Foundation of China (91027041, 21090343, 21390404, and 51373193), and the Chinese Academy of Sciences.

■ REFERENCES

(1) Balzani, V.; Credi, A.; Venturi, M. *ChemSusChem* **2008**, *1*, 26.
(2) Lubitz, W.; Reijerse, E. J.; Messinger, J. *Energy Environ. Sci.* **2008**, *1*, 15.
(3) Magnuson, A.; Anderlund, M.; Johansson, O.; Lindblad, P.; Lomoth, R.; Polivka, T.; Ott, S.; Stensjö, K.; Styring, S.; Sundström, V.; Hammarström, L. *Acc. Chem. Res.* **2009**, *42*, 1899.
(4) Frischmann, P. D.; Mahata, K.; Wurthner, F. *Chem. Soc. Rev.* **2013**, *42*, 1847.
(5) Nocera, D. G. *Acc. Chem. Res.* **2012**, *45*, 767.
(6) Wang, H.-Y.; Wang, W.-G.; Si, G.; Wang, F.; Tung, C.-H.; Wu, L.-Z. *Langmuir* **2010**, *26*, 9766.
(7) Zhu, L.; Khairutdinov, R. F.; Cape, J. L.; Hurst, J. K. *J. Am. Chem. Soc.* **2005**, *128*, 825.
(8) Sasaki, R.; Nako, Y.; Murata, S. *Tetrahedron* **2009**, *65*, 7364.
(9) Watanabe, K.; Moriya, K.; Kouyama, T.; Onoda, A.; Minatani, T.; Takizawa, S.-y.; Murata, S. *J. Photochem. Photobiol., A* **2011**, *221*, 113.
(10) Sun, J.; Zhang, J.; Zhang, M.; Antonietti, M.; Fu, X.; Wang, X. *Nat. Commun.* **2012**, *3*, 1139.
(11) Wang, D.; Hisatomi, T.; Takata, T.; Pan, C.; Katayama, M.; Kubota, J.; Domen, K. *Angew. Chem., Int. Ed.* **2013**, *52*, 11252.
(12) Li, Z.-J.; Li, X.-B.; Wang, J.-J.; Yu, S.; Li, C.-B.; Tung, C.-H.; Wu, L.-Z. *Energy Environ. Sci.* **2013**, *6*, 465.
(13) Zeng, H. C. *J. Mater. Chem.* **2011**, *21*, 7511.
(14) Lou, X. W.; Archer, L. A.; Yang, Z. *Adv. Mater.* **2008**, *20*, 3987.
(15) Liu, J.; Liu, F.; Gao, K.; Wu, J.; Xue, D. *J. Mater. Chem.* **2009**, *19*, 6073.
(16) Hu, J.; Chen, M.; Fang, X.; Wu, L. *Chem. Soc. Rev.* **2011**, *40*, 5472.
(17) Lai, X.; Halpert, J. E.; Wang, D. *Energy Environ. Sci.* **2012**, *5*, 5604.
(18) Srivastava, S.; Santos, A.; Critchley, K.; Kim, K.-S.; Podsiadlo, P.; Sun, K.; Lee, J.; Xu, C.; Lilly, G. D.; Glotzer, S. C.; Kotov, N. A. *Science* **2010**, *327*, 1355.
(19) King'ondu, C. K.; Iyer, A.; Njagi, E. C.; Opembe, N.; Genuino, H.; Huang, H.; Ristau, R. A.; Suib, S. L. *J. Am. Chem. Soc.* **2011**, *133*, 4186.
(20) Bai, F.; Sun, Z.; Wu, H.; Haddad, R. E.; Xiao, X.; Fan, H. *Nano Lett.* **2011**, *11*, 3759.
(21) Kamat, P. V. *J. Phys. Chem. C* **2008**, *112*, 18737.
(22) Kamat, P. V.; Tvrdy, K.; Baker, D. R.; Radich, J. G. *Chem. Rev.* **2010**, *110*, 6664.
(23) Greene, B. L.; Joseph, C. A.; Maroney, M. J.; Dyer, R. B. *J. Am. Chem. Soc.* **2012**, *134*, 11108.

(24) Brown, K. A.; Dayal, S.; Ai, X.; Rumbles, G.; King, P. W. *J. Am. Chem. Soc.* **2010**, *132*, 9672.
(25) Wang, F.; Wang, W.-G.; Wang, X.-J.; Wang, H.-Y.; Tung, C.-H.; Wu, L.-Z. *Angew. Chem., Int. Ed.* **2011**, *50*, 3193.
(26) Nann, T.; Ibrahim, S. K.; Woi, P. M.; Xu, S.; Ziegler, J.; Pickett, C. J. *Angew. Chem., Int. Ed.* **2010**, *49*, 1574.
(27) Huang, J.; Mulfort, K. L.; Du, P.; Chen, L. X. *J. Am. Chem. Soc.* **2012**, *134*, 16472.
(28) Han, Z.; Qiu, F.; Eisenberg, R.; Holland, P. L.; Krauss, T. D. *Science* **2012**, *338*, 1321.
(29) Yang, D.; Wang, F.; Yan, J.; Gao, Y.; Li, H. *J. Nanopart. Res.* **2013**, *15*, 1.
(30) Li, Z.-J.; Wang, J.-J.; Li, X.-B.; Fan, X.-B.; Meng, Q.-Y.; Feng, K.; Chen, B.; Tung, C.-H.; Wu, L.-Z. *Adv. Mater.* **2013**, *25*, 6613.
(31) Wang, J.-J.; Li, Z.-J.; Li, X.-B.; Fan, X.-B.; Meng, Q.-Y.; Yu, S.; Li, C.-B.; Li, J.-X.; Tung, C.-H.; Wu, L.-Z. *ChemSusChem* **2014**, *7*, 1468.
(32) Wang, F.; Liang, W.-J.; Jian, J.-X.; Li, C.-B.; Chen, B.; Tung, C.-H.; Wu, L.-Z. *Angew. Chem., Int. Ed.* **2013**, *52*, 8134.
(33) Li, C.-B.; Li, Z.-J.; Yu, S.; Wang, G.-X.; Wang, F.; Meng, Q.-Y.; Chen, B.; Feng, K.; Tung, C.-H.; Wu, L.-Z. *Energy Environ. Sci.* **2013**, *6*, 2597.
(34) Jian, J.-X.; Liu, Q.; Li, Z.-J.; Wang, F.; Li, X.-B.; Li, C.-B.; Liu, B.; Meng, Q.-Y.; Chen, B.; Feng, K.; Tung, C.-H.; Wu, L.-Z. *Nat. Commun.* **2013**, *4*, 2695.
(35) Yin, Y.; Rioux, R. M.; Erdonmez, C. K.; Hughes, S.; Somorjai, G. A.; Alivisatos, A. P. *Science* **2004**, *304*, 711.
(36) Bhattacharyya, J.; Das, S.; Mukhopadhyay, S. *Dalton Trans.* **2007**, 1214.
(37) Rogach, A. L. *Mater. Sci. Eng., B* **2000**, *69*−*70*, 435.
(38) Li, L.; Qian, H.; Fang, N.; Ren, J. *J. Lumin.* **2006**, *116*, 59.
(39) Chen, J. L.; Zheng, A. F.; Gao, Y. C.; He, C. Y.; Wu, G. H.; Chen, Y. C.; Kai, X. M.; Zhu, C. Q. *Spectrochim. Acta, Part A* **2008**, *69*, 1044.
(40) Bao, H.; Gong, Y.; Li, Z.; Gao, M. *Chem. Mater.* **2004**, *16*, 3853.
(41) Sarma, D. D.; Santra, P. K.; Mukherjee, S.; Nag, A. *Chem. Mater.* **2013**, *25*, 1222.
(42) Kulkarni, S. K.; Winkler, U.; Deshmukh, N.; Borse, P. H.; Fink, R.; Umbach, E. *Appl. Surf. Sci.* **2001**, *169*−*170*, 438.
(43) Hutchison, J. E.; Postlethwaite, T. A.; Murray, R. W. *Langmuir* **1993**, *9*, 3277.
(44) Reiss, P.; Bleuse, J.; Pron, A. *Nano Lett.* **2002**, *2*, 781.
(45) Huang, X.; Li, G.; Cao, B.; Wang, M.; Hao, C. *J. Phys. Chem. C* **2009**, *113*, 4381.
(46) Zhang, W.; Wang, Y.; Wang, Z.; Zhong, Z.; Xu, R. *Chem. Commun.* **2010**, *46*, 7631.
(47) Dong, C.; Qian, H.; Fang, N.; Ren, J. *J. Phys. Chem. B* **2006**, *110*, 11069.
(48) Nag, A.; Chung, D. S.; Dolzhnikov, D. S.; Dimitrijevic, N. M.; Chattopadhyay, S.; Shibata, T.; Talapin, D. V. *J. Am. Chem. Soc.* **2012**, *134*, 13604.
(49) Kovalenko, M. V.; Scheele, M.; Talapin, D. V. *Science* **2009**, *324*, 1417.
(50) Sun, Q.; Ren, Z.; Wang, R.; Wang, N.; Cao, X. *J. Mater. Chem.* **2011**, *21*, 1925.
(51) Chuang, C.-H.; Burda, C. *J. Phys. Chem. Lett.* **2012**, *3*, 1921.
(52) Pradhan, N.; Battaglia, D. M.; Liu, Y.; Peng, X. *Nano Lett.* **2006**, *7*, 312.
(53) Aldana, J.; Lavelle, N.; Wang, Y.; Peng, X. *J. Am. Chem. Soc.* **2005**, *127*, 2496.
(54) Zhang, Y.; Mi, L.; Wang, P. N.; Ma, J.; Chen, J. Y. *J. Lumin.* **2008**, *128*, 1948.
(55) Susha, A. S.; Javier, A. M.; Parak, W. J.; Rogach, A. L. *Colloids Surf., A* **2006**, *281*, 40.
(56) Xu, S.; Wang, C.; Xu, Q.; Zhang, H.; Li, R.; Shao, H.; Lei, W.; Cui, Y. *Chem. Mater.* **2010**, *22*, 5838.
(57) Zhu, H.; Song, N.; Lv, H.; Hill, C. L.; Lian, T. *J. Am. Chem. Soc.* **2012**, *134*, 11701.
(58) Creutz, C. *Inorg. Chem.* **1981**, *20*, 4449.
(59) Aquilano, D.; Costa, E.; Genovese, A.; Roberto Massaro, F.; Pastero, L.; Rubbo, M. *J. Cryst. Growth* **2003**, *247*, 516.
(60) Fan, X.; Zhang, Z.; Li, G.; Rowson, N. A. *Chem. Eng. Sci.* **2004**, *59*, 2639.
(61) Liu, J.; Xue, D. *J. Cryst. Growth* **2009**, *311*, 500.
(62) Peng, Q.; Dong, Y.; Li, Y. *Angew. Chem., Int. Ed.* **2003**, *42*, 3027.
(63) Zhang, H.; Zhang, S.; Pan, S.; Li, G.; Hou, J. *Nanotechnology* **2004**, *15*, 945.
(64) Jiang, C.; Zhang, W.; Zou, G.; Yu, W.; Qian, Y. *Nanotechnology* **2005**, *16*, 551.
(65) Li, X.; Xiong, Y.; Li, Z.; Xie, Y. *Inorg. Chem.* **2006**, *45*, 3493.
(66) Wang, W.; Zhang, P.; Peng, L.; Xie, W.; Zhang, G.; Tu, Y.; Mai, W. *CrystEngComm* **2010**, *12*, 700.
(67) Wang, H.; Liang, J.; Fan, H.; Xi, B.; Zhang, M.; Xiong, S.; Zhu, Y.; Qian, Y. *J. Solid State Chem.* **2008**, *181*, 122.
(68) Zhang, H.; Zhou, Z.; Yang, B.; Gao, M. *J. Phys. Chem. B* **2002**, *107*, 8.